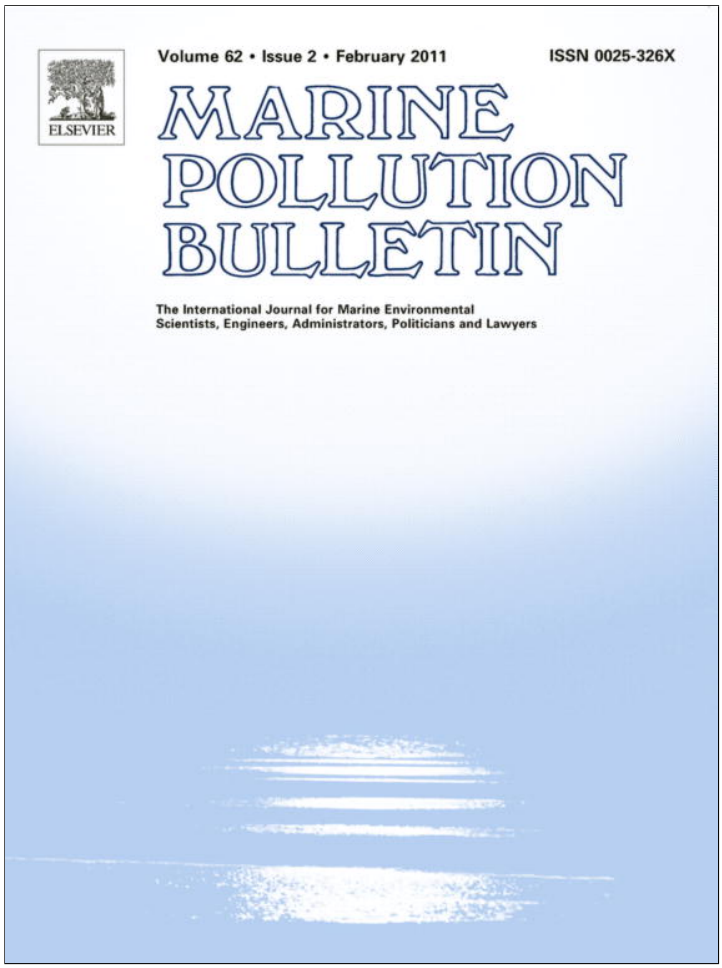

Marine Pollution Bulletin 62 (2011) 350–363

Contents lists available at ScienceDirect

Marine Pollution Bulletin

journal homepage: www.elsevier.com/locate/marpolbul

# SAR observation and model tracking of an oil spill event in coastal waters

Yongcun Cheng [a,*], Xiaofeng Li [b], Qing Xu [c,d,e], Oscar Garcia-Pineda [f], Ole Baltazar Andersen [a], William G. Pichel [g]

[a] DTU Space, National Space Center, Juliane Mariesvej 30, Copenhagen 2100, Denmark
[b] IMSG at NOAA/NESDIS, Camp Springs, MD 20746, USA
[c] State Key Laboratory of Hydrology-Water Resources and Hydraulic Engineering, Hohai University, Nanjing 210098, China
[d] Key Laboratory of Coastal Disaster and Defense, Ministry of Education, Hohai University, Nanjing 210098, China
[e] LASG, Institute of Atmospheric Physics, Chinese Academy of Science, Beijing 100029, China
[f] Florida State University, 117 N. Woodward Avenue, Tallahassee, FL, USA
[g] NOAA/NESDIS/STAR, Camp Springs, MD 20746, USA

ARTICLE INFO

*Keywords:*
Oil spill
GNOME
Trajectory
SAR
Simulation

ABSTRACT

Oil spills are a major contributor to marine pollution. The objective of this work is to simulate the oil spill trajectory of oil released from a pipeline leaking in the Gulf of Mexico with the GNOME (General NOAA Operational Modeling Environment) model. The model was developed by NOAA (National Oceanic and Atmospheric Administration) to investigate the effects of different pollutants and environmental conditions on trajectory results. Also, a Texture-Classifying Neural Network Algorithm (TCNNA) was used to delineate ocean oil slicks from synthetic aperture radar (SAR) observations. During the simulation, ocean currents from NCOM (Navy Coastal Ocean Model) outputs and surface wind data measured by an NDBC (National Data Buoy Center) buoy are used to drive the GNOME model. The results show good agreement between the simulated trajectory of the oil spill and synchronous observations from the European ENVISAT ASAR (Advanced Synthetic Aperture Radar) and the Japanese ALOS (Advanced Land Observing Satellite) PALSAR (Phased Array L-band Synthetic Aperture Radar) images. Based on experience with past marine oil spills, about 63.0% of the oil will float and 18.5% of the oil will evaporate and disperse. In addition, the effects from uncertainty of ocean currents and the diffusion coefficient on the trajectory results are also studied.



## 1. Introduction

Pollution of the ocean by mineral, or petroleum, oil is a major environmental problem (Alpers and Espedal, 2004). Cargo ships and pipelines submerged in the marine environment carry huge amounts of petroleum across the open ocean and in coastal areas (Verma et al., 2008). Annually, 48% of the oil pollution in the oceans is fuel oil and 29% is crude oil (Brekke and Solberg, 2005). Accurate detection and forecast of oil spill trajectory would be beneficial to fisheries, wildlife, and resource management for monitoring and conserve of the marine environment. It is one of the most important applications for operational oceanography (Hackett et al., 2009).

For oil detection, ocean remote sensing data, especially SAR (synthetic aperture radar) data, have been used to provide valuable synoptic information about the position and size of the oil spill due to its wide area coverage and day/night, and all-weather capabilities. Many efforts have been undertaken to obtain statistical information on oil pollution from SAR images (Gade and Alpers, 1999; Lu et al., 1999, 2000; Lu, 2003; Brekke and Solberg, 2008; Ferraro et al., 2009; Garcia-Pineda et al., 2009).

For oil spill tracking, ocean drift models are often used. These models are usually driven by a time series of ocean currents, ocean surface wind vectors, sea surface temperature, etc. An overview of oil spill models is given by Galt (1994), Reed et al. (1999) and Hackett et al. (2006). In general, commonly used operational oil spill models include GNOME (General NOAA Operational Modeling Environment, http://response.restoration.noaa.gov/), MOTHY (French operational oil spill drift forecast system, http://www.meteorologie.eu.org/mothy/), OSCAR (Oil Spill Contingency and Response, http://www.sintef.no), ADIOS2 (Automated Data Inquiry for Oil Spills, http://response.restoration.noaa.gov), OILMAP (Oil Spill Model and Response System, http://www.aims.gov.au/pages/research/oil-map/oil-map01.html) and OSIS (Oil Spill Identification System, http://www.osis.biz/ss2.asp). Among the various oil spill models, the GNOME model supports the NOAA/National Ocean Service (NOS), Office of Response an Restoration (OR&R), Emergency

* Corresponding author.
*E-mail address:* cych@space.dtu.dk (Y. Cheng).

0025-326X/$ - see front matter © 2010 Elsevier Ltd. All rights reserved.
doi:10.1016/j.marpolbul.2010.10.005

Response Division (ERD) standard for best guess and minimum regret trajectories by providing information about where the spill is most likely to go (Best Guess Solution) and the uncertainty bound (Minimum Regret Solution) (Beegle-Krause, 2001). Compared with other models, the GNOME model can be used anywhere in the world and requires fewer input parameters than most other models.

In operational use, after the oil spill information is obtained from SAR images, the GNOME model can be run in near-real time for the prediction of oil spill trajectories. In this way, the simulation results can be used by the authorities to respond quickly in order to decrease the pollution's impact on the marine environment. Bergueiro López et al. (2006) used the EUROSPILL, OILMAP, GNOME and ADIOS models in simulating an oil spill at the Casablanca Platform (Tarragona, Spain) under a variety of environmental conditions. The values of the evaporated fraction versus time obtained with the GNOME model are most accurate when using proposed polynomial equations of second and third order. The GNOME model is also used to investigate the effects of different pollutants and environmental conditions on trajectory results, e.g., for cyanobacterial bloom transport (Wynne et al., 2010, personal communication) and larval dispersal (Engie and Klinger, 2007).

In this work, the GNOME model is used to simulate and predict the trajectory of oil released from a pipeline in the Gulf of Mexico (the position of the pipeline is shown in Fig. 1) on July 26, 2009. The detection of oil slicks from SAR observations are based on the method proposed by Garcia-Pineda et al. (2009). The simulation results are compared with a time series of European Space Agency (ESA) ENVISAT ASAR (Advanced SAR) and Japanese ALOS (Advanced Land Observing Satellite) PALSAR (Phased Array L-Band Synthetic Aperture Radar) images. The paper is organized in the following way: in Section 2, we will introduce the GNOME model and the input parameters. Section 3 contains simulation results and verification. The effects of uncertainties on the oil spill trajectory are also shown in this section. The conclusions are given in Section 4.

## 2. Methodology

### 2.1. GNOME model

The GNOME model was developed by the NOAA/ERD (Emergency Response Division) in the Office of Response and Restoration (OR&R). NOAA OR&R ERD has employed GNOME as a nowcast/forecast model primarily in pollution transport analyses for many years. The system provides the capability of experimenting with oil spill behavior under different weather conditions. GNOME utilizes the NOAA CATS (Current Analysis for Trajectory Simulation) model for dispersion. In GNOME, the produced "splots" (called Lagrangian/Eulerian (continuous) elements or LEs) are a collection of point representations that collectively indicate the extent of spilled oil (Beegle-Krause, 2001, 2003, 2005).

The movement of the splots is either to remain on the water, to be beached, to be weathered and disappear or to travel out of the modeling space domain. Different types of splots are represented in different ways. In any trajectory that includes a "minimum regret solution", black splots represent GNOME's best guess of where spilled oil will go. (For all black splots, wind and model data are assumed to be correct.) Red splots represent the "minimum regret" area for the same spill. When splots are beached, the "best guess" splots are shown as black "x"s; beached "minimum regret" splots are shown as red "x"s (NOAA, 2002).

GNOME estimates oil spill movement using a combination of default and user-supplied information on ocean winds, currents and oil characteristics. It supports two different user modes. In standard/GIS mode, regionally-specific location files use questions to guide users in setting up their scenarios. The diagnostic mode enables users to set up custom trajectory models that can accept circulation patterns from any hydrodynamic model, provided the model output is in a GNOME-readable format. The GNOME diagnostic mode includes the ability to construct movie visualizations

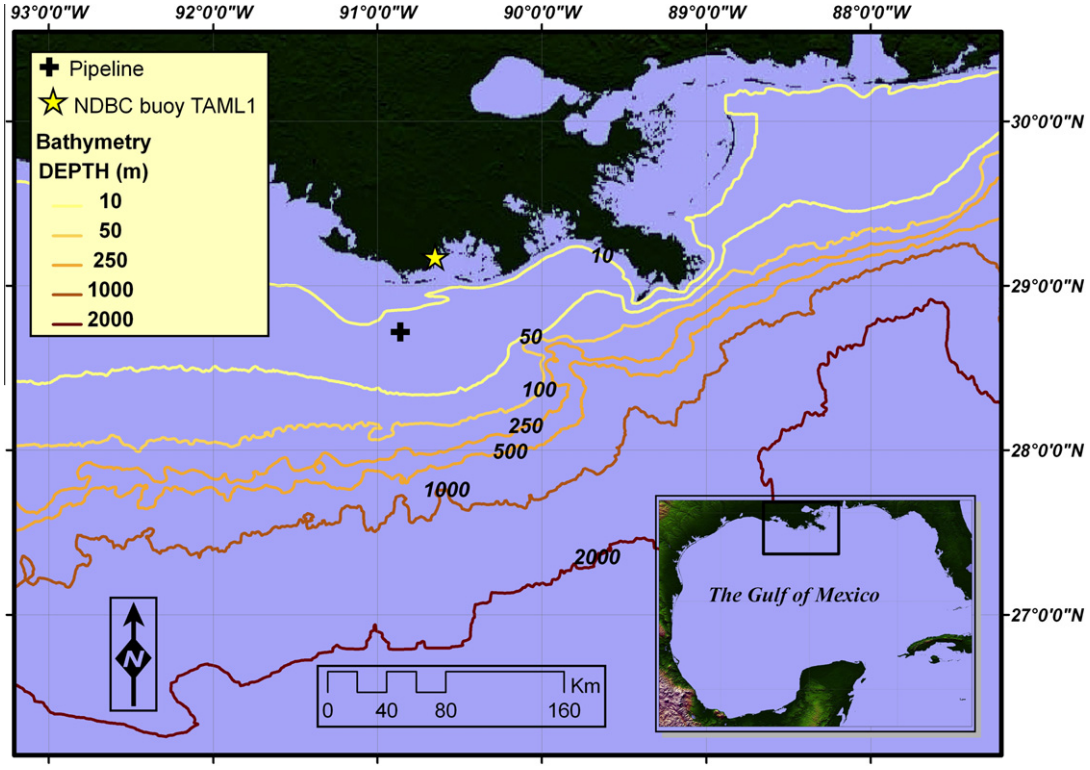


**Fig. 1.** Study area. Locations of the pipeline (28.7135N, 90.8698W) and NDBC buoy TAML1 (29.188N, 90.665W) in the Gulf of Mexico are shown as plus and star, respectively. The solid lines show the topography of the research area (the data are from ETOPO2v2 Global Gridded 2-min Database, National Geophysical Data Center, National Oceanic and Atmospheric Administration, US Dept. of Commerce, http://www.ngdc.noaa.gov/mgg/global/etopo2.html).

showing oil spill trajectory across a given seascape. Users can define a polygon and input a series of splots into the model; the splots movement will be simulated through time.

Best Guess and Minimum Regret trajectories calculated by GNOME are also considered standard products by NOAA. The Best Guess trajectory represents the most likely movement path of the spill, whereas the Minimum Regret trajectory provides an uncertainty bound (NASA, 2004). All simulations presented in this study were run in GNOME version 1.3.0 using the diagnostic mode. The ocean surface currents data are obtained from NCOM (Navy Coastal Ocean Model) outputs and ocean surface winds are measurements from a nearby NDBC (National Data Buoy Center) buoy.

### 2.2. Data and model setting

#### 2.2.1. SAR observations

In this work, observations from ENVISAT ASAR and ALOS PALSAR are available. Information on three SAR images is given in Table 1. The European Space Agency (ESA) ENVISAT satellite was launched in March 2002. It operates in C-band with different polarization combinations. Important new capabilities of ASAR include beam steering for acquiring images with different incidence angles, dual polarization and wide swath coverage. Users have access to a variety of beam selections that can image swaths from 56 to 405 km in width, with resolutions from 30 to 150 m and at incidence angles from 15° to 45°. ALOS was launched by the Japan Aerospace Exploration Agency (JAXA) in January 2006. It operates in L-band with different polarization combinations. The spatial resolution of the ALOS PALSAR is 7–88 m for the Fine resolution mode and 100 m for the ScanSAR mode. The observation swath is 40–70 km for Fine mode and 250–350 km for ScanSAR mode.

In the work of Garcia-Pineda et al. (2009), they developed a Texture-Classifying Neural Network Algorithm (TCNNA), which processes SAR data from a wide selection of beam modes, to extract oil spill/seep patterns from SAR imagery in a semi-supervised procedure. The algorithm uses a combination of edge detection filters, descriptors of texture, collection information (e.g., beam mode), and environmental data, which is processed with a neural network. From experience with the TCNNA and from the results of other SAR research, it has been found that the optimum wind range to study surfactant films is from 3.5 to 7.0 m $s^{-1}$. In our study, the TCNNA was used to detect oil spill information in SAR images.

Fig. 2a shows all the available SAR observations listed in Table 1. The oil spills detected in these images using the TCNNA are shown in Fig. 2b. In this figure, the movements and the oil spill distribution characteristics are shown clearly. In the first 24 h, the oil spill disperses and the distribution area enlarges from 3.06 to 9.73 $km^2$. After 60 h, the spilled oil moved 32 km towards the northeast, and the area of oil spill area decreases from 9.73 to 5.85 $km^2$.

Fig. 2c and d shows the selected oil spill in the ENVISAT ASAR image acquired on July 26, 2009 and its detection results with the TCNNA, respectively. The length of the oil spill is about 10 km. The beginning time of oil spill trajectory simulation was set as 16:10 UTC, July, 26, which is quite close to the observation time. The time step was 10 min. Fig. 2e shows the oil spill in another ENVISAT ASAR image acquired on July 29, 2009. Fig. 2f shows the detailed distribution of the oil spill detected with the TCNNA. The shape of oil spill has changed to a belt. Its length is about 6 km. The observation time of this image is set as the ending time of the oil spill trajectory simulation. In addition, ALOS SAR also observed the oil spill on July 27, 2009 (Fig. 2g and h). It can be seen that the oil did not migrate from the position of the pipeline and that the length of oil spill is about 24 km. From the shape of oil spill in Fig. 2h, it can be concluded that the pipeline may still have been leaking oil at this time. All these SAR observations are used to verify the simulation results.

#### 2.2.2. Ocean currents

For any model, reliable environmental observations and predictions are the basis for an accurate prediction of the oil spill trajectory. Such data provide an overall picture of meteorological and oceanographic conditions. In order to simulate the movement of the oil spill detected in the SAR images, we need ocean wind and current inputs to force the GNOME model. In the literatures, Elhakeem et al. (2007) use a hydrodynamic model (MIKE3-HD) and oil spill model (MIKE3-SA) to simulate an oil spill trajectory in the Arabian Gulf successfully. After that, the MIKE 21 model was used to simulate a diesel oil spill in the Arabian Gulf (Verma et al., 2008). Guo and Wang (2009) developed a hybrid particle-tracking Eulerian–Lagrangian approach for the simulation of spilled oil in coastal areas. To acquire accurate environmental information, the oil model they proposed is coupled with a 3-D free-surface hydrodynamics model (POM) and a third-generation wave model (SWAN). It was also pointed out by Hackett et al. (2009) that the ability to monitor and predict marine oil spills depends on access to high-quality information on ocean circulation.

In this manuscript, ocean currents in the Gulf of Mexico were obtained from a 3-D hydrodynamic model, NCOM, which is maintained by NRL (Navy Research Laboratory). It is the first operational global ocean model that outputs ocean currents, temperature, salinity, sea surface height and other parameter (Barron et al., 2007). The global NCOM is run daily at the Naval Oceanographic Office (http://www7320.nrlssc.navy.mil/global_ncom/).

The NCOM model uses 41 $\sigma$–$z$ layers, among them 19 are $\sigma$-coordinate layers in the upper 137 m, and 21 are $z$-coordinate layers from 137 to 5500 m. The surface layer ocean currents are used in the GNOME model. The spatial resolution of NCOM is 1/8° and the temporal resolution is 3 h. Time variations of currents are calculated based on start time and the run duration that entered in the GNOME model (GNOME user manual, 2002). The oil spill observed in this case study is from July 26 to July 29, 2009. Therefore, the NCOM forecast results of ocean currents from 15:00 UTC on July 26 to 06:00 UTC on July 29, 2009 are used to force the GNOME model. Fig. 3 shows the ocean currents close to the SAR imaging time described in Table 1. Fig. 3a–d are forecast current fields at 15:00 UTC on July 26, 15:00 UTC on July 27, 03:00 UTC on July 28, and 03:00 UTC on July 29, respectively. In the Gulf of Mexico, diurnal tides predominate so that the ocean current patterns between Fig. 3a, b and c, d are similar.

#### 2.2.3. Winds

In addition to ocean currents, surface wind is another important input parameter for the GNOME model. In this study, similar to the work in Wynne et al. (2010, personal communication), the hourly 10-m wind measurements from NDBC buoy TAML1 (shown by a

**Table 1**
Information of SAR images used in this study.

| No. | Time | SAR image | Satellite | SAR mode | Polarization | Band | Resolution (m) | Swath (km) |
|---|---|---|---|---|---|---|---|---|
| 1 | 16:10:33 UTC 07/26/2009 | ASAR | ENVISAT | Wide Swath | VV | C | 150 | 400 |
| 2 | 16:32:53 UTC 07/27/2009 | PALSAR | ALOS | ScanSAR | HH | L | 100 | 350 |
| 3 | 03:57:49 UTC 07/29/2009 | ASAR | ENVISAT | Wide Swath | VV | C | 150 | 400 |

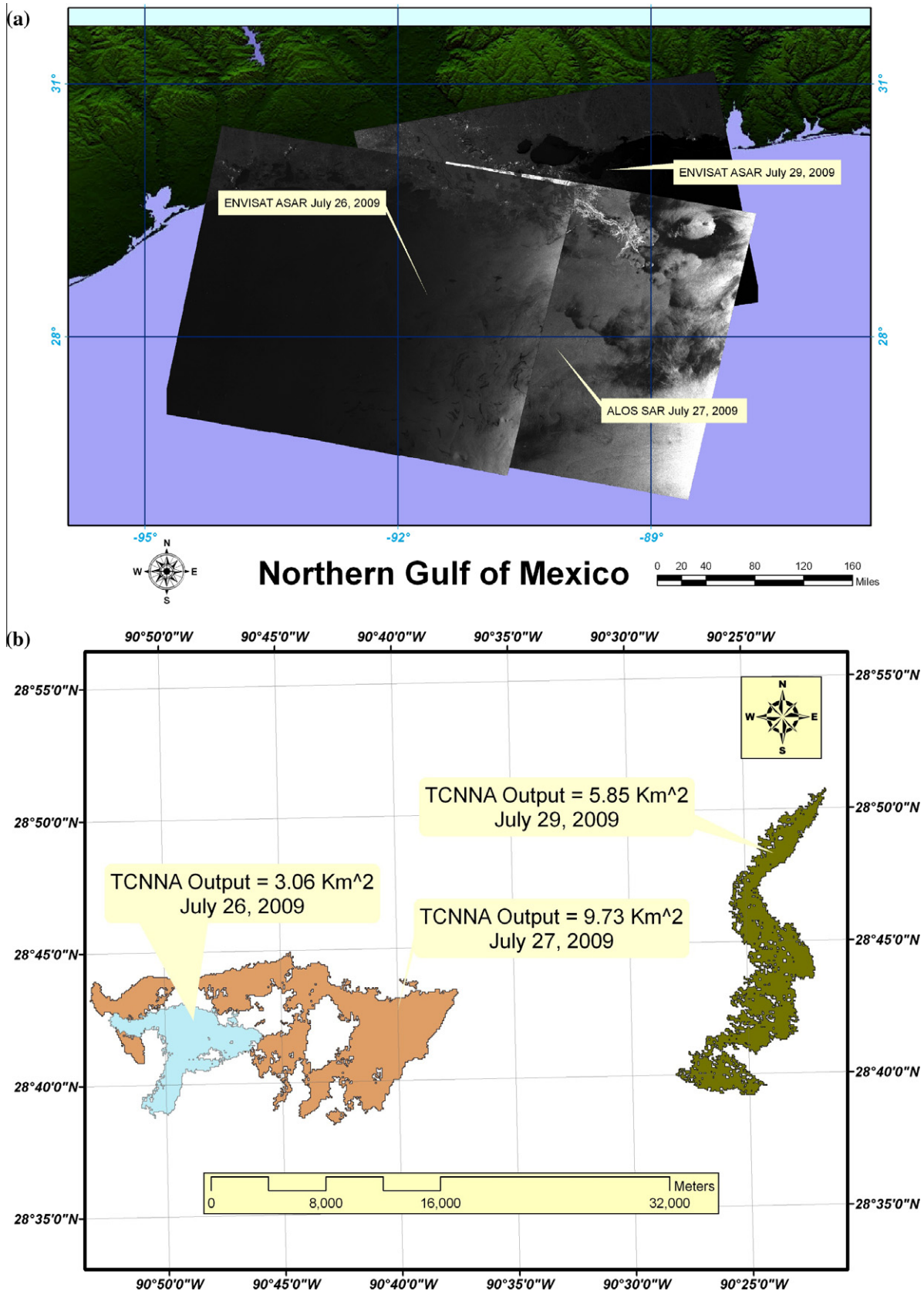


**Fig. 2.** Oil spill detected from SAR images: (a) all available SAR observations; (b) detected oil spill information with TCNNA for the different times listed in Table 1; (c) enlarged subset image of oil spill acquired on July 26, 2009; (d) the detected results based on SAR image (c) and TCNNA; (e) enlarged subset image of oil spill acquired on July 29, 2009; (f) the detected results based on SAR image (e) and TCNNA; (g) enlarged subset image of oil spill acquired on July 27, 2009; (h) the detected results based on SAR image (g) and TCNNA.

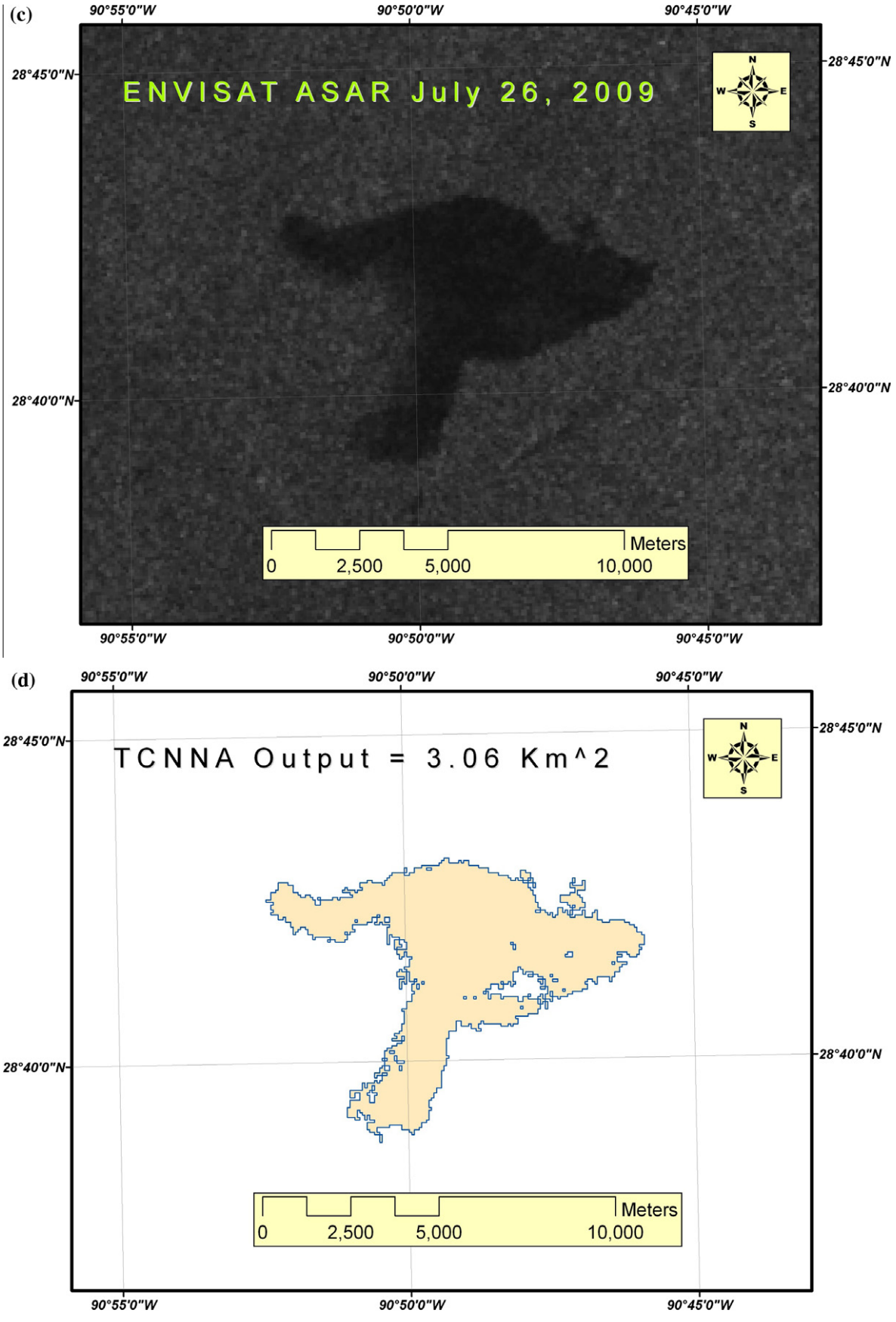


**Fig. 2** (*continued*)

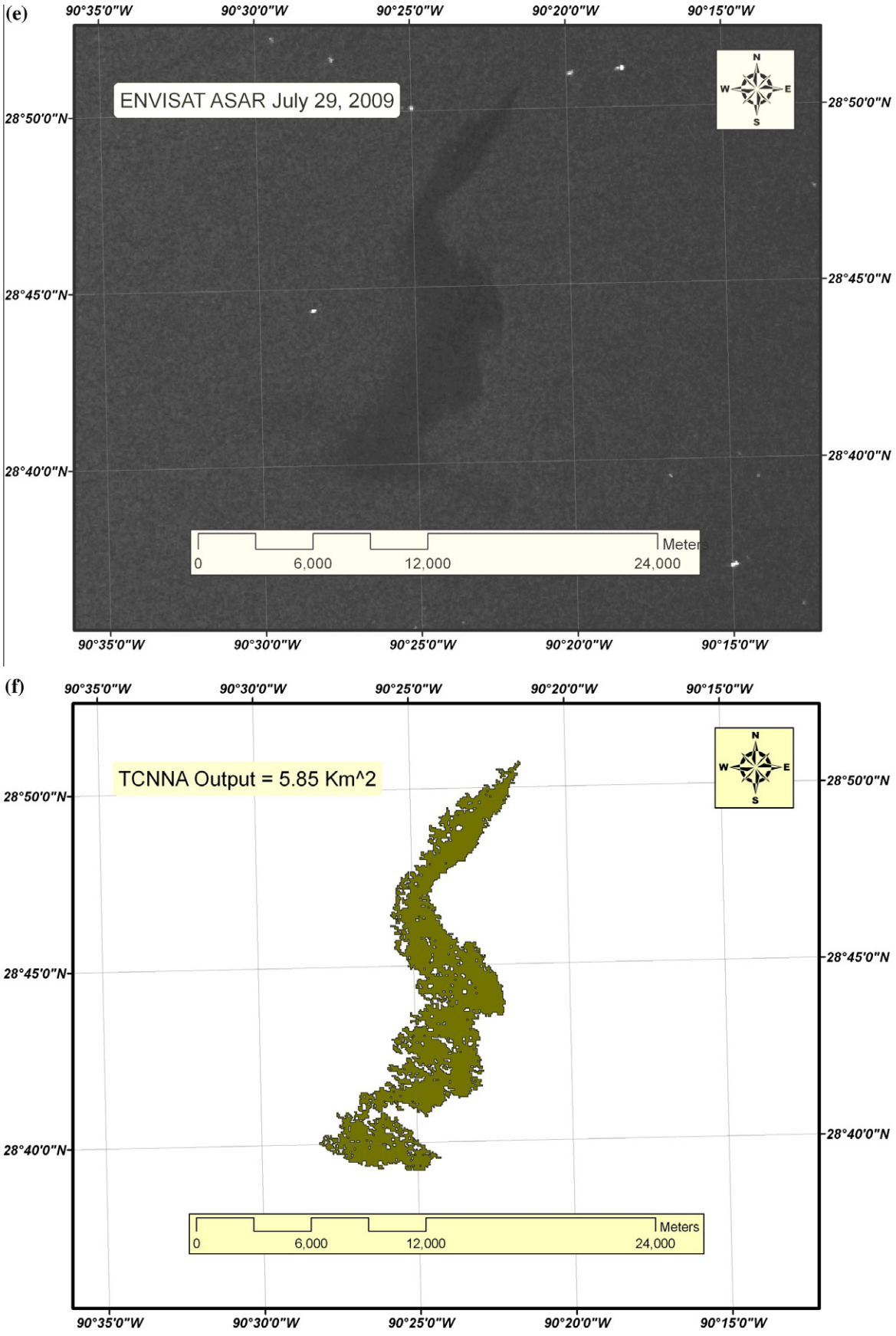


**Fig. 2** (*continued*)

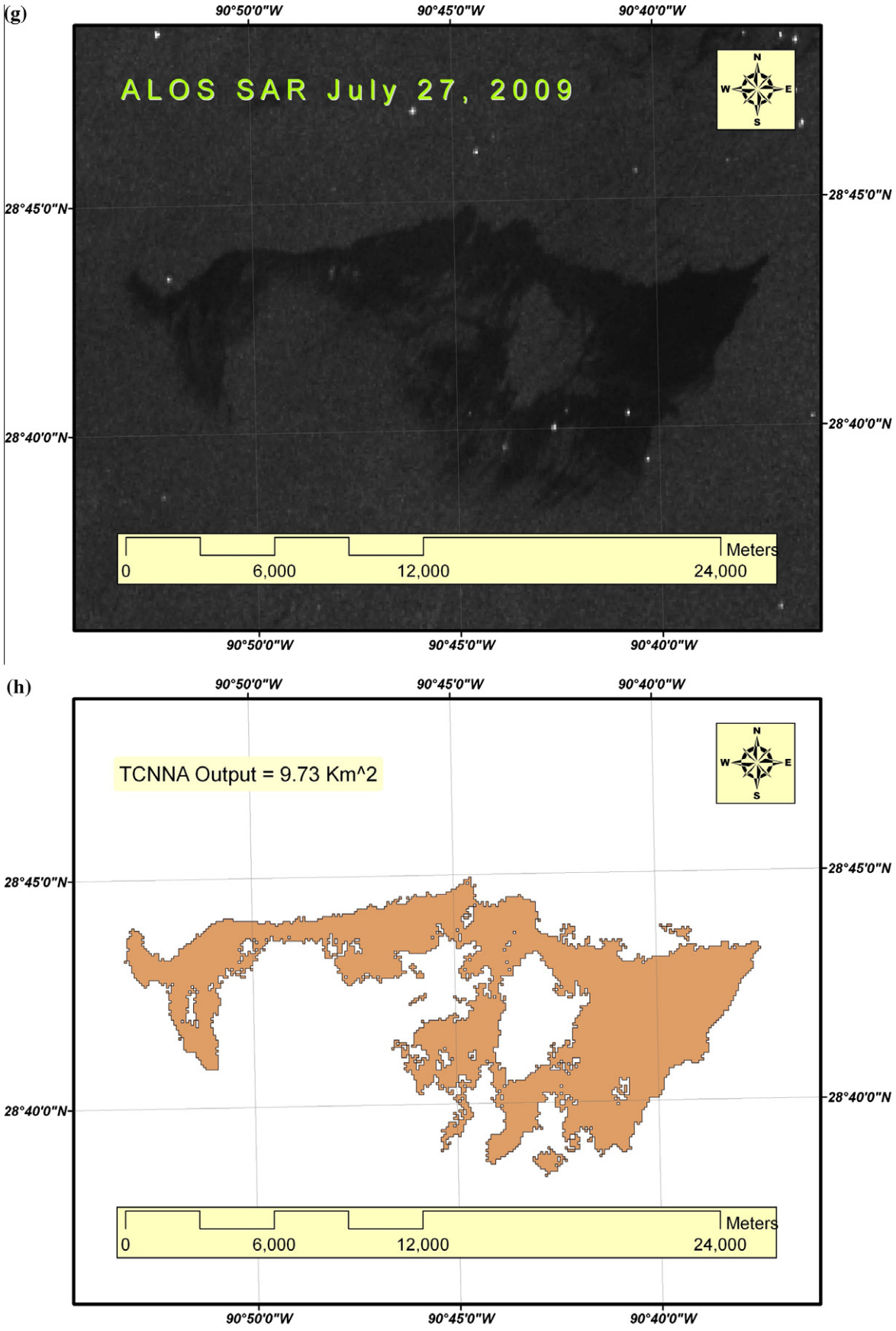


**Fig. 2** (*continued*)

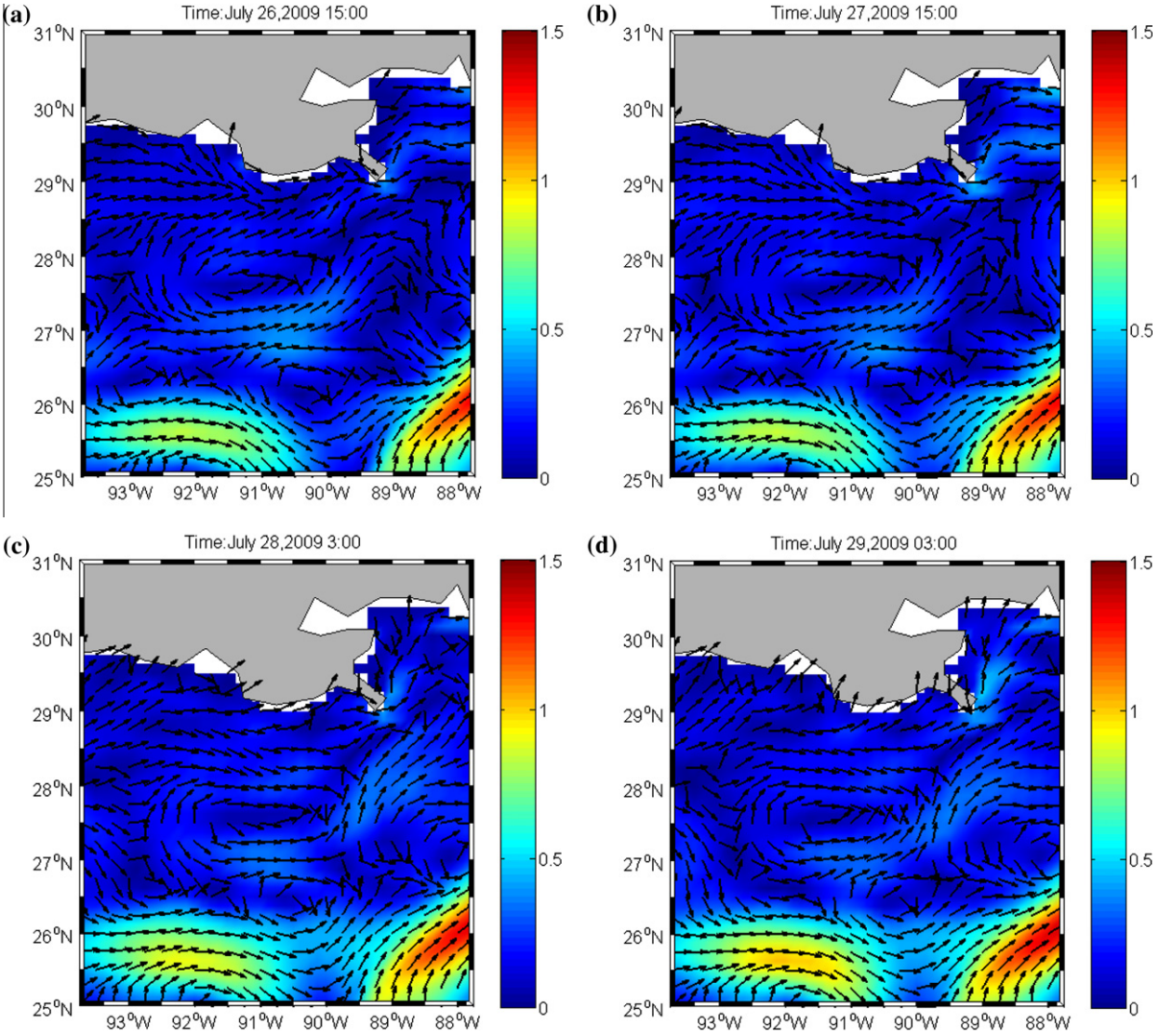


**Fig. 3.** NCOM forecast ocean current fields at times near the SAR observation time: (a) at 15:00 UTC on July 26, 2009; (b) at 15:00 UTC on July 27, 2009; (c) at 03:00 UTC on July 28, 2009; and (d) at 03:00 UTC on July 29, 2009.

star in Fig. 1) are used to force the GNOME model. Fig. 4 shows a time series of wind vectors plotted from July 26 to July 30, 2009. During this period, the winds are light, blowing toward the northeast with speeds less than 7.7 m/s. This wind condition is conducive to oil patch detection using SAR because higher winds will break the surface oil film. The TCNNA also performs well with this wind condition.

*2.2.4. Model setting*

Due to uncertainly of NCOM ocean current error, we run GNOME with the minimum uncertainty error of 1% for ocean current speed in both along-current and cross-current directions. GNOME allows users to select different types of weathering or non-weathering for different types of spills, i.e., gasoline, diesel, medium crude and fuel oil. In this study, weathering for crude oil is selected. We assume the amount of oil spilled is 50 barrels and the shape of the oil spill is extracted from the SAR images. This amount of oil corresponds to 200 splots in the model domain. These splots are given a release time equal to the overpass time of the first SAR image, and a time series of NCOM current fields and the winds are input to the GNOME model to perform the simulation. The oil spill pattern in the GNOME model is shown in Fig. 5 with 200 blue solid points. As one can see, the solid points are sprayed with almost the same pattern as that of the oil spill shown on the ENVISAT ASAR image from July 26, 2009 (Fig. 2c).

If the current and wind predictions are accurate, and if the windage (i.e., how much force the wind exerts on the oil to move it in the direction that the wind is blowing) and diffusion parameters are set accurately in GNOME, then GNOME will generate very good trajectories. In this study, it was assumed that both the measured wind from the buoy and the NCOM output currents are accurate. The windage is set as 0–1% and the minimum uncertainty error of both along-current and cross-current directions are set as 1% in magnitude. The diffusion coefficient and its uncertainty factor are set as 100,000 $cm^2\ s^{-1}$ and 1, respectively, which are default setting and minimum value in GNOME.

## 3. Results and discussion

### 3.1. Simulation results

The Best Guess Solution of GNOME is created by assuming no errors in wind and current inputs (Beegle-Krause, 2003). This

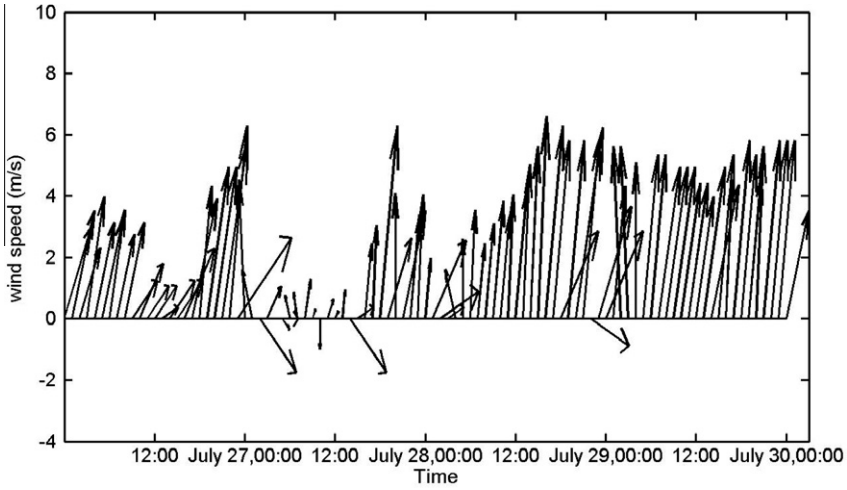


**Fig. 4.** Ocean surface wind fields measured from NDBC buoy station TAML1.

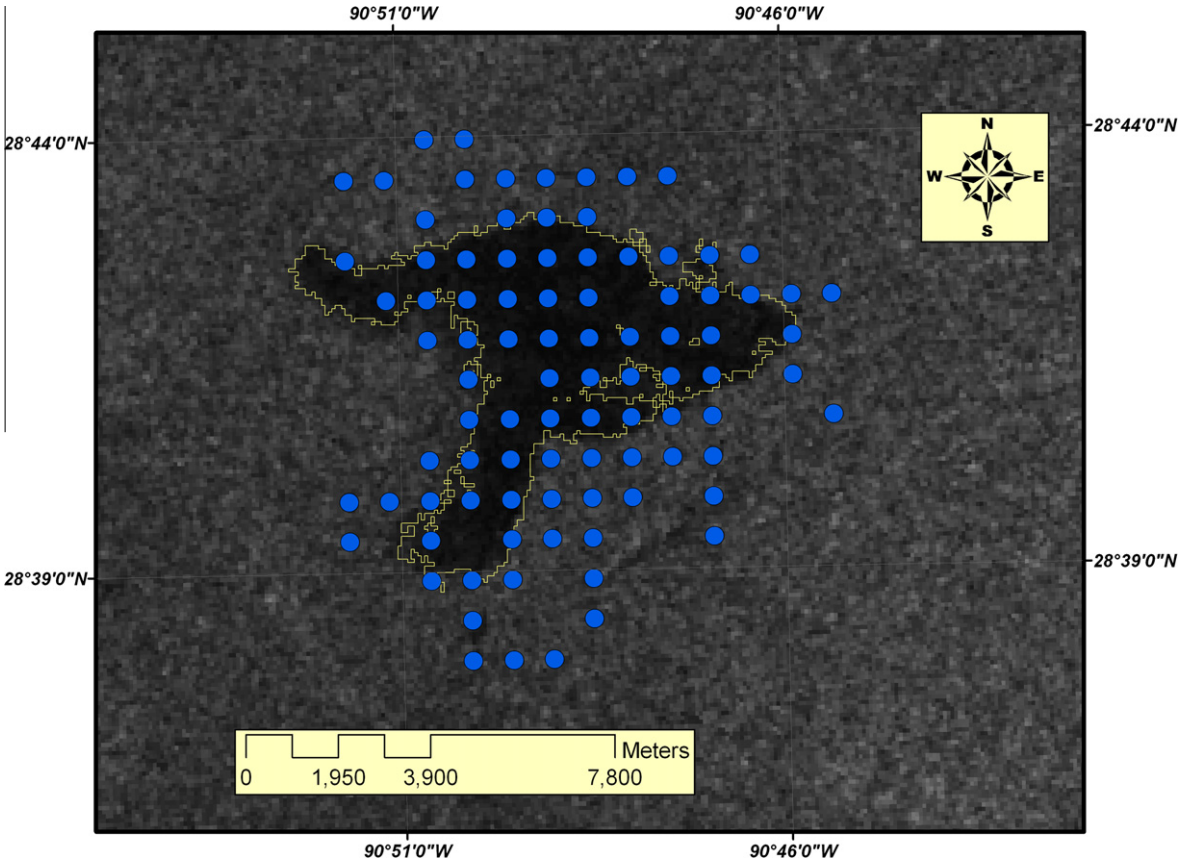


**Fig. 5.** Initial oil spill distribution denoted by blue spots. The yellow lines denote edge of oil spill detected with TCNNA.

solution is also known as the forecast trajectory. This trajectory represents the best guess of where spilled oil will go. We run the GNOME model starting at 16:10 UTC on July 26, 2009, and continue running for 60 h with 10 min time steps.

Comparisons between the simulated trajectory of the oil spill and the SAR observations are shown in Fig. 6. The blue solid points (i.e., the original splots, now translated to their new positions by the GNOME model denote the most probable area (Best Guess Solution) that the oil will pollute. Fig. 6a and b shows the actual locations of the oil spill and simulated positions of the splots as determined by the GNOME model at 16:30 UTC on July 27 and 04:00 UTC on July 29, 2009, respectively. Compared with the SAR observations, after the first 24 h run of the model, the simulated oil-polluted area coincides with the synchronous PALSAR observation well (Fig. 6a). It also can be seen from Fig. 6a that some of the area is not coved by the supposed spray solid points. There are two reasons responsible for the results. First, the pipeline may still be spilling oil during the simulation, and this cannot be simulated within the model. Secondly, we supposed that all the input parameters were accurate and the uncertainties of wind speed and ocean

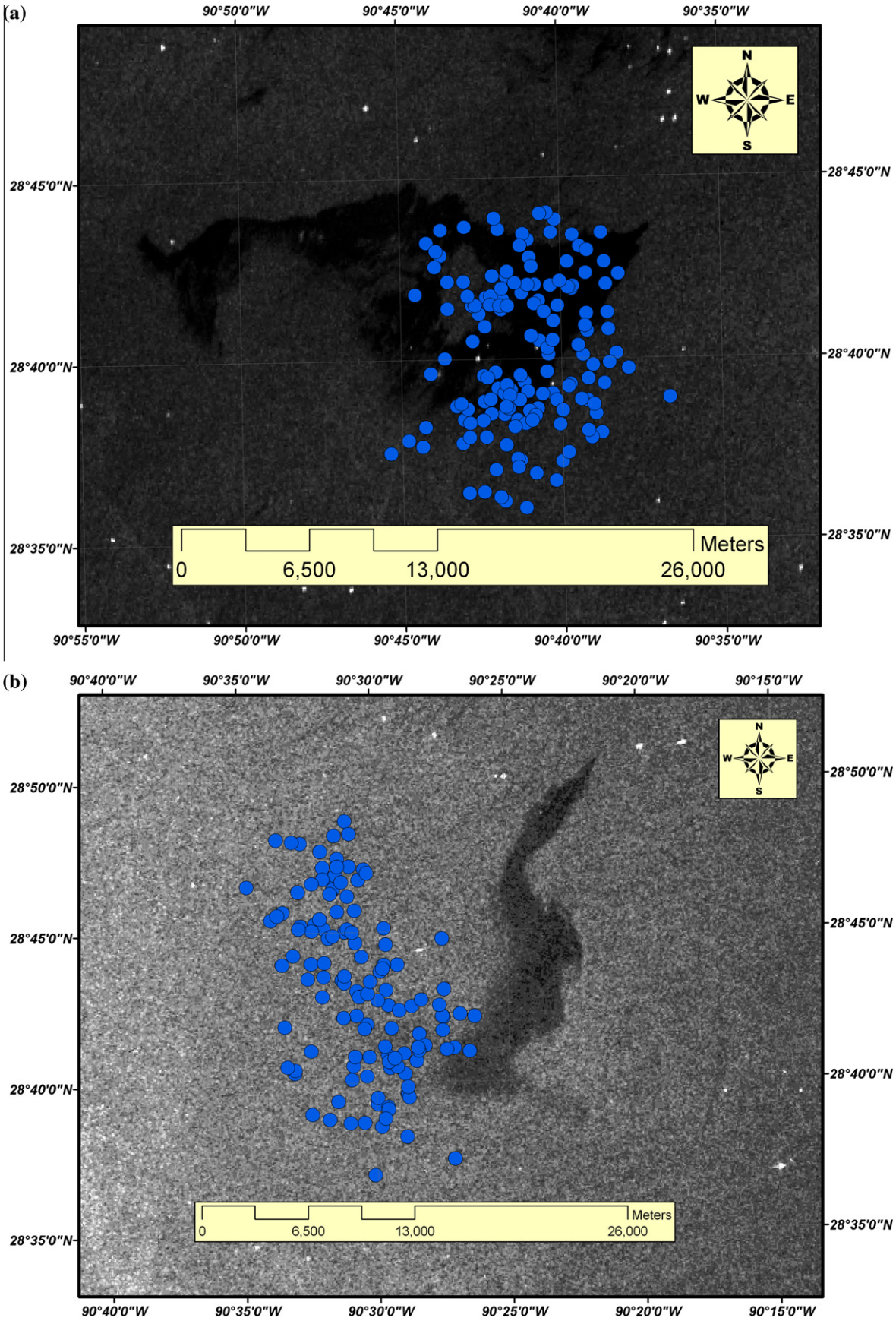


**Fig. 6.** GNOME simulated best guess trajectory of oil spill denoted by blue solid points: (a) at 16:30 UTC on July 27, 2009; and (b) at the ending of the simulation, 04:00 UTC on July 29, 2009.

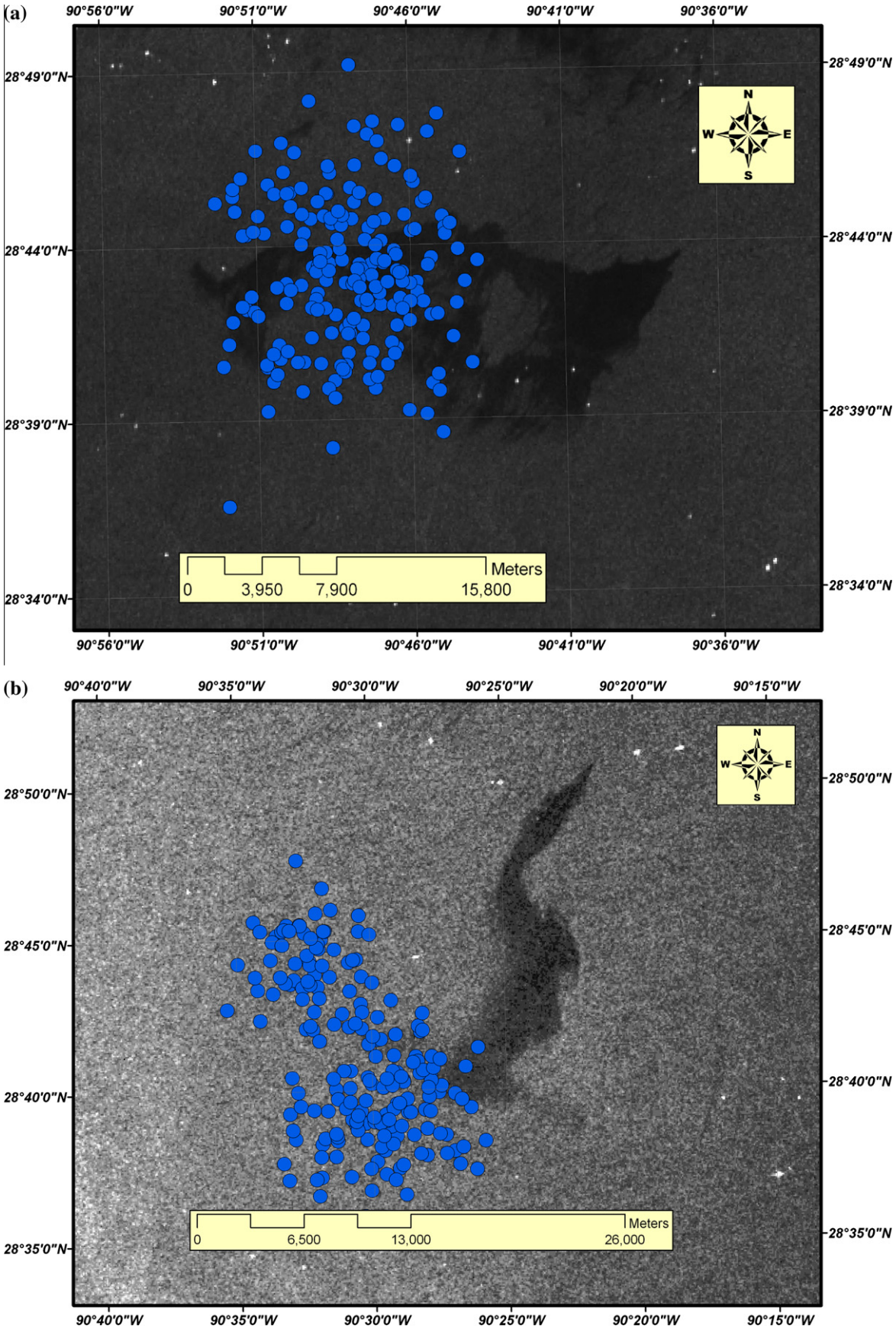


**Fig. 7.** GNOME simulated locations of the oil spill at 04:00 UTC on July 29, 2009: (a) with only using wind to force the model; and (b) with only using the currents to force the model.

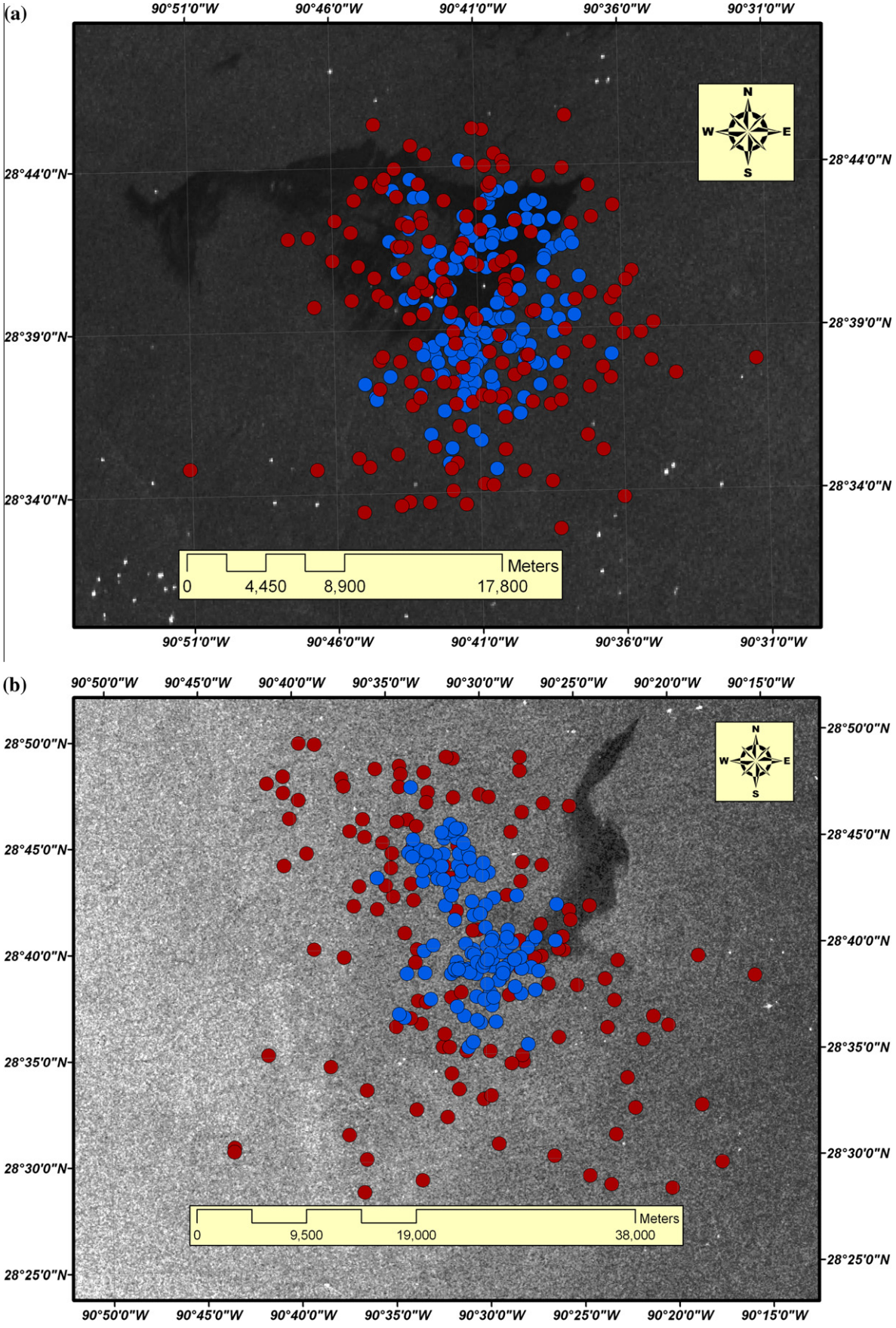


**Fig. 8.** Effects of uncertainties on oil spill simulation results which are denoted by red solid points: (a) at 16:30 UTC on July 27, 2009; and (b) at 04:00 UTC on July 29, 2009. The blue solid points denote the Best Guess Solution of the GNOME model.

currents were not included. Fig. 6b is a comparison between simulated results and the synchronous ENVISAT ASAR observation (Fig. 2e and f). After the GNOME model run of 60 h, the observed oil spill was not covered by the simulated most probable area. The model did not translate the splots as far to the east as the movement of the actual oil spill. This could be caused by uncertainties in the input parameters, which will be discussed in Section 3.2. In general, the shape of the simulation is similar to the actual spill observation. Based on the GNOME calculation, about 63.0% of the oil will float and 18.5% of the oil will evaporate and disperse.

We run GNOME with separate wind and ocean current inputs to determine the dominate factor forcing the oil drift. Fig. 7a and b are projected locations of the oil spill at 04:00 UTC on July 29, 2009 when separately using only currents and only winds, respectively to force the model. It can be seen clearly from Fig. 7a that all splots (denoted by blue solid points) move around the initial spill area when only winds are used to drive the model. It was found that, compared with ocean currents, the contribution of wind speed and wind direction to the movement of oil spill is smaller.

### 3.2. Uncertainty analysis

It is common to incorporate uncertainties in the input data to provide error-bounds to help with interpretation of outputs from oil spill models. The actual concentration of dispersed oil in the water column is also expected to have a large variability around the estimated mean concentration (Mearns et al., 2001). Sebastião and Guedes Soares (2007) introduced a method to account for the uncertainties in the predictions of oil spill trajectories using a classic oil spill model. In the OILMAP and GNOME models, multiple particles are used to account for these uncertainties by calculating spill trajectories for each of the many particles. The trajectories are affected by random variations, within a user-defined range, on the "best estimates" of currents and wind speed (Lehr et al., 1999, 2003). This procedure results in a wider predicted spill path and thus provides a more conservative estimate of the locations that could be exposed (APASA, 2003).

The Minimum Regret Solution of GNOME is a statistical trajectory compilation that attempts to add error into the forecast trajectory by uncertainty terms. Users can define ocean current speed uncertainty in error percentage in both along-current and cross-current directions. From Fig. 1 it can be seen that in the simulated area, the bathymetry is between 10 and 20 m. Since the simulated area is close to the coast, the uncertainty of ocean currents from forecast models may be large due to the complicity of shoreline and bottom bathymetry. To describe the effects of uncertainties on GNOME simulations, we set both along-current uncertainty and cross-current uncertainty of ocean current speed as 50%. The other uncertainty factor is the diffusion coefficient. For a given condition of wind speed and ocean currents, if the coefficient is large enough, the splots may be transported to the beach. In this section, we set the diffusion coefficient and its uncertainty factor as 100,000 $cm^2\ s^{-1}$ and 5, respectively. The uncertainty of wind speed is set to 1–3%, which is in the normal value range.

The GNOME model uses these inputs to simultaneously run 1000 separate splots to sample the uncertainty. Each of these uncertainty splots samples a different portion of the uncertainty space. The trajectories of these uncertainty splots map the domain for the Minimum Regret Solution to calculate the uncertainty boundary for the trajectory (Beegle-Krause, 2001). Fig. 8 shows the comparisons between simulation results at 16:30 UTC on July 27 and 04:00 UTC on July 29, 2009 with synchronous observations, respectively. The blue and red solid points denote the Best Guess Solution and the Minimum Regret Solution of GNOME, respectively. Compared with results in Fig. 6, with the added uncertainty factors, the polluted areas simulated with the GNOME model agree quite well with the measurements during the 60-h model run (Fig. 8b).

## 4. Conclusions

In this work, an oil spill event from a pipeline leaking in the Gulf of Mexico was observed by spaceborne SAR sensors onboard both the ENVISAT and ALOS satellites in July 2009. A neural-network-based oil spill detection algorithm is used to derive the oil spill information from these three SAR images. The NOAA operational oil spill model, GNOME, was used to simulate an oil spill accident in the Gulf of Mexico. The ocean current fields from NCOM and wind fields measured from a nearby NDBC buoy station were used to force the model. The oil spill observations from the ENVISAT ASAR and the ALOS SAR images were used to determine the oil spill information and verify the simulation results. The comparisons at different times show good agreements between model simulation and SAR observations. Compared with other meteorological and oceanographic factors, the ocean current fields play the most important role in driving the movement of the oil spill. To get more accurate simulation results from the GNOME model, the effects of uncertainty in ocean currents and in the diffusion coefficient were analyzed. After considering the uncertainty factors, the polluted areas simulated with the GNOME model agree well with the measurements.

## Acknowledgments

We thank Robert Daniels (NOAA/NCEP/Ocean Prediction Center) for providing NCOM forecast ocean current outputs. SAR images were provided by ESA through Envisat projects 431 and 6133, and by the Japan Aerospace Exploration Agency (JAXA), the University of Miami Center for Southeastern Tropical Advanced Remote Sensing and the University of Alaska, Fairbanks Alaska Satellite Facility through ALOS Project 51 (First Research Announcement). This work was also supported by National Natural Science Foundation of China (Grant No. 41006108), the Open Fund of State Key Laboratory of Satellite Ocean Environment Dynamics (Grant No. SOED0909), the Fundamental Research Funds for the Central Universities (Grant No. 2009B02514), the Knowledge Innovation Program of the Chinese Academy of Sciences (Grant No. IAP09316) and the Special Fund of State Key Laboratory of Hydrology-Water Resources and Hydraulic Engineering. The views, opinions, and findings contained in this report are those of the authors and should not be construed as an official NOAA or US Government position, policy, or decision.

## References

Alpers, W.H., Espedal, A., 2004. Oils and surfactants. In: Christopher, R.J., Apel, J.R. (Eds.), Synthetic Aperture Radar Marine User's Manual. US Department of Commerce, Washington, DC, pp. 263–276.

Asia Pacific Applied Science Associates and the Ecology Lab Pty. Ltd., 2003. A Review of Recent Innovations and Current Research in Oil and Chemical Spill Technology. Technical Report, p. 82. Available online: <http://www.amsa.gov.au/marine_environment_protection/National_Plan/Contingency_Plans_and_Management/Research_Development_and_Technology/Spill_ Technology.pdf>.

Barron, C.N., Kara, A.B., Rhodes, R.C., Rowley, C., Smedstad, L.F., 2007. Validation Test Report for the 1/8 Global Navy Coastal Ocean Model Nowcast/Forecast System. NRL Technical Report. NRL/MR/7320-07-9019.

Beegle-Krause, C.J., 2001. General NOAA oil modeling environment (GNOME): a new spill trajectory model. International Oil Spill Conference, 865–871.

Beegle-Krause, C.J., 2003. Advantages of separating the circulation model and trajectory model: GNOME trajectory model used with outside circulation. In: Environment Canada Arctic and Marine Oil Spill Program Technical Seminar (AMOP) Proceedings, vol. 26 (2), pp. 825–840.

Beegle-Krause, C.J., 2005. General NOAA oil modeling environment (GNOME): a new spill trajectory model. In: International Oil Spill Conference. IOSC 2005, pp. 3277–3283.

Bergueiro López, J.R., Romero March, R., Guijarro González, S., Serra Socías, F., 2006. Simulation of oil spills at the Casablanca Platform (Tarragona, Spain)

under different environmental conditions. Journal of Maritime Research 3 (1), 55–72.
Brekke, C., Solberg, A.H.S., 2005. Oil spill detection by satellite remote sensing. Remote Sensing of Environment. doi:10.1016/j.rse.2004.11.015.
Brekke, C., Solberg, A.H.S., 2008. Classifiers and confidence estimation for oil spill detection in ENVISAT ASAR images. IEEE Geoscience and Remote Sensing Letters 5 (1), 65–69.
Elhakeem, A.A., Elshorbagy, W., Chebbi, R., 2007. Oil spill simulation and validation in the Arabian (Persian) Gulf with special reference to the UAE coast. Water, Air, and Soil Pollution 184, 243–254.
Engie, K., Klinger, T., 2007. Modeling passive dispersal through a large estuarine system to evaluate marine reserve network connections. Estuaries and Coasts 30 (2), 201–213.
European Space Agency, 2007. ASAR Product Handbook. European Space Agency-ENVISAT Product Handbook, Technical Report. Issue 2.2, 27 February 2007.
Ferraro, G., Meyer-Roux, S., Muellenhoff, O., Pavliha, M., Svetak, J., Tarchi, D., Topouzelis, K., 2009. Long term monitoring of oil spills in European seas. International Journal of Remote Sensing 30 (3), 627–645.
Gade, M., Alpers, W., 1999. Using ERS-2 SAR for routine observation of marine pollution in European coastal waters. Science of the Total Environment 237–238, 441–448.
Galt, J.A., 1994. Trajectory analysis for oil spills. Journal of Advanced Marine Technology Conference 11, 91–126.
Garcia-Pineda, O., Zimmer, B., Howard, M., Pichel, W., Li, X.F., MacDonald, I.R., 2009. Using SAR image to delineate ocean oil slicks with a texture classifying neural network algorithm (TCNNA). Canadian Journal of Remote Sensing 35 (5), 411–421.
GNOME user manual, 2002. Available online: <http://response.restoration.noaa.gov/book_shelf/711_GNOME_Manual.pdf>, p. 17.
Guo, W.J., Wang, Y.X., 2009. A numerical oil spill model based on a hybrid method. Marine Pollution Bulletin 58, 726–734.
Hackett, B., Breivik, Ø., Wettre, C., 2006. Forecasting the drift of objects and substances in the ocean. In: Chassignet, E.P., Verron, J. (Eds.), Ocean Weather Forecasting, An Integrated View of Oceanography. Springer, Dordrecht, pp. 507–524.
Hackett, B., Comerma, E., Daniel, P., Ichikawa, H., 2009. Marine oil pollution prediction. Oceanography 22 (3), 168–175.
Lehr, W., Barker, C., Simecek-Beatty, D., 1999. New developments in the use of uncertainty in oil spill forecasts. In: Proceedings of the 22nd Arctic and Marine Oilspill Program Technical Seminar. Alberta, Canada, pp. 271–284.
Lehr, W.J., Simecek-Beatty, D., Hodges, M., 2003. Wind uncertainty in long-range trajectory forecasts. In: Proceedings of the 2003 International Oil Spill Conference. British Columbia, Canada.
Lu, J., 2003. Marine oil spill detection, statistics and mapping with ERS SAR imagery in south-east Asia. International Journal of Remote Sensing 24 (15), 3013–3032.
Lu, J., Lim, H., Liew, S.C., Bao, M., Kwoh, L.K., 1999. Statistics in Southeast Asian waters compiled from ERS synthetic aperture radar imagery. Earth Observation Quarterly 621, 13–17.
Lu, J., Kwoh, L.K., Lim, H., Liew, S.C., Bao, M., 2000. Mapping oil pollution from space. Backscatter 11, 23–26.
Mearns, A., Watabayashi, G., Lankford, J., 2001. Dispersing oil near shore in the California current region. CalCOFI Report, vol. 42.
NASA Report, 2004. Decision Support Tool Evaluation Report for GNOME, Version 2.0, p. 65.
NOAA Users Manual, 2002. General NOAA Oil Modeling Environment. NOAA Office of Response and Restoration, Hazardous Materials Response Division, p. 91.
Reed, M., Johansen, Ø., Brandvik, P.J., Daling, P.S., Lewis, A., Fiocco, R., Mackay, D., Prentki, R., 1999. Oil spill modeling towards the close of the 20th century: overview of the state of the art. Spill Science and Technology Bulletin 5 (1), 3–16.
Sebastião, P., Guedes Soares, C., 2007. Uncertainty in predictions of oil spill trajectories in open sea. Ocean Engineering 34, 576–584.
Verma, P., Wate, S.R., Devotta, S., 2008. Simulation of impact of oil spill in the ocean – a case study of Arabian Gulf. Environmental Monitoring and Assessment 146, 191–201.
Wynne, T.T., Stumpf, R.P., Tomlinson, M.C., Schwab, D.J., personal communication. Ecological forecasting: estimating cyanobacterial bloom 1 transport with remotely sensed imagery and a hydrodynamic model.